Exact Solution of the Bose-Hubbard Model with Unidirectional Hopping

Mingchen Zheng,[1,2] Yi Qiao[3] Yupeng Wang,[1] Junpeng Cao,[1,2,4,5] and Shu Chen[1,2,*]

[1]*Beijing National Laboratory for Condensed Matter Physics, Institute of Physics, Chinese Academy of Sciences, Beijing 100190, China*
[2]*School of Physical Sciences, University of Chinese Academy of Sciences, Beijing 100049, China*
[3]*Institute of Modern Physics, Northwest University, Xi'an 710127, China*
[4]*Songshan lake Materials Laboratory, Dongguan, Guangdong 523808, China*
[5]*Peng Huanwu Center for Fundamental Theory, Xian 710127, China*

A one-dimensional Bose-Hubbard model with unidirectional hopping is shown to be exactly solvable. Applying the algebraic Bethe ansatz method, we prove the integrability of the model and derive the Bethe ansatz equations. The exact eigenvalue spectrum can be obtained by solving these equations. The distribution of Bethe roots reveals the presence of a superfluid-Mott insulator transition at the ground state, and the critical point is determined. By adjusting the boundary parameter, we demonstrate the existence of a non-Hermitian skin effect even in the presence of interaction, but it is completely suppressed for the Mott insulator state in the thermodynamical limit. Our result represents a new class of exactly solvable non-Hermitian many-body systems, which has no Hermitian correspondence and can be used as a benchmark for various numerical techniques developed for non-Hermitian many-body systems.

Introduction.—Exact solutions of integrable quantum many-body models, e.g., the Lieb-Liniger model [1,2], Yang-Gaudin model [3,4], and Fermi Hubbard model [5], provide crucial insights into the understanding of correlation effect and have wide application in cold atomic and condensed matter physics [6]. However, constructing a new quantum integrable model with simple form and clear physical meanings is a difficult and fascinating mission. Recently, a great deal of progress has been made in the theory of non-Hermitian physics [7–10]. Some novel phenomena such as the enriched non-Hermitian topological classification [11–16], non-Hermitian skin effect (NHSE) [17–22], and scale-free localization [23–27] have attracted intensive studies. At present, most novel phenomena and concepts about the non-Hermitian effects are built based on noninteracting systems. Then it is necessary to demonstrate whether these concepts are applicable and what new effect arises when the interaction is considered. Recently, there is attracting growing interest in exploring non-Hermitian phenomena in many-body systems, e.g., the interplay of non-Hermitian skin effect and interaction [28–30], the fate of the correlated phase in the presence of non-Hermiticity [28,31–35], and non-Hermitian topological phases in correlated systems [36–38].

Most of the existing studies on the non-Hermitian many-body systems are carried out by numerical diagonalization, which suffers from the many-body exponential wall problem and the problem of numerical errors and calculation precision in the diagonalization of non-Hermitian systems [39,40]. The current understanding of NHSE and scale-free localization in correlated systems is quite limited.

Exact solutions of non-Hermitian integrable many-body systems can provide benchmarks for understanding novel phenomena due to the interplay of non-Hermiticity and interaction. In this work, we propose an integrable non-Hermitian Bose-Hubbard model describing the interacting bosons in a chain with unidirectional hopping, which is one of the conserved quantities constructed from the expansion coefficients of transfer matrix, whose integrability is guaranteed by the Yang-Baxter equation. It is well known that the Bose-Hubbard model is not integrable and cannot be analytically solved [41,42]. Compared to the previously reported exactly solvable non-Hermitian many-body systems [31,32,43–46], whose integrability is inherited from their Hermitian corresponding models by either introducing an imaginary gauge field or complex continuation of parameters, our model is a new integrable system without a Hermitian counterpart. By using an algebraic Bethe ansatz method [47,48], we exactly solve the model and obtain the exact energy spectrum. Although the spectrum of a non-Hermitian many-body system is generally complex, we find that the ground state (defined by the minimum of real parts of eigenvalues) of our model is real. We unveil the occurrence of a superfluid-Mott insulator transition for integer filling cases by adjusting the ratio of interaction strength and hopping amplitude. Additionally, based on the obtained exact eigenstates, we also demonstrate the existence of a non-Hermitian skin effect even in the presence of interaction, which is, however, found to be completely suppressed for the Mott state in the thermodynamical limit.

Model and its exact solution.—The model Hamiltonian reads

$$H = -t\left[\sum_{j=1}^{N-1} b_j^\dagger b_{j+1} + \epsilon b_N^\dagger b_1\right] + \frac{U}{2}\sum_{j=1}^{N} n_j(n_j - 1), \quad (1)$$

where $b_j^\dagger$ and b_j are bosonic creation and annihilation operators at jth site, respectively, $n_j = b_j^\dagger b_j$ is the particle number operator on the jth site, N is the number of sites, t quantifies the hopping between two sites with the nearest neighbor, ϵ is the boundary parameter, and U characterizes the strength of on-site interaction. For simplicity, we consider $t > 0$ and the on-site interaction is repulsive, i.e., $U > 0$. Since the Hamiltonian includes only a unidirectional hopping term, it is a non-Hermitian model.

First, we prove that the model (1) is integrable in the framework of the quantum inverse scattering method [47]. A series of conserved quantities of the Hamiltonian (1) can be generated by a transfer matrix

$$t(u) = \mathrm{tr}_0[L_{0,N}(u)L_{0,N-1}(u)\ldots L_{0,1}(u)K_0], \quad (2)$$

where u is the spectral parameter, tr_0 means the trace in the two-dimensional auxiliary space V_0, the subscripts $\{1,\ldots,N\}$ denote the physical spaces, $L_{0,j}(u)$ is the Lax operator defined in the tensor space $V_0 \otimes V_j$, and K_0 is the 2×2 diagonal matrix given by $K_0 = \mathrm{diag}(1, \epsilon)$. In the auxiliary space, the Lax operator can be expressed by the matrix

$$L_{0,j}(u) = \begin{pmatrix} u - n_j & gb_j \\ gb_j^\dagger & -g^2 \end{pmatrix}, \quad (3)$$

where the elements are the bosonic operators defined in the jth site and g is a constant. The Lax operator (3) satisfies the Yang-Baxter relation

$$R_{0,\bar{0}}(u-v)L_{0,j}(u)L_{\bar{0},j}(v) = L_{\bar{0},j}(v)L_{0,j}(u)R_{0,\bar{0}}(u-v), \quad (4)$$

where $R_{0,\bar{0}}(u)$ is the R matrix defined in the auxiliary spaces 0 and $\bar{0}$ with the form of

$$R_{0,\bar{0}}(u) = \begin{pmatrix} u-1 & 0 & 0 & 0 \\ 0 & u & -1 & 0 \\ 0 & -1 & u & 0 \\ 0 & 0 & 0 & u-1 \end{pmatrix}. \quad (5)$$

Using the Yang-Baxter relation (4), it can be proven that the transfer matrices with different spectral parameters commute with each other, i.e., $[t(u), t(v)] = 0$. Expanding the transfer matrix $t(u)$ with respect to u,

$$t(u) = u^N + C_1 u^{N-1} + C_2 u^{N-2} + \cdots, \quad (6)$$

then all the expansion coefficients C_n $(n = 1, \ldots, N)$ are commutative and can be taken as conserved quantities.

Choosing one of them or a certain combination of them as a Hamiltonian H, then $[H, C_n] = 0$ and the model is integrable. Direct calculation gives the operators C_1 and C_2 as

$$C_1 = -\sum_{j=1}^{N} n_j, \quad (7)$$

$$C_2 = \frac{1}{2}\sum_{i\neq j}^{N} n_i n_j + g^2\left(\sum_{j=1}^{N-1} b_j^\dagger b_{j+1} + \epsilon b_N^\dagger b_1\right). \quad (8)$$

The integrable Hamiltonian (1) is constructed as

$$H = \frac{t}{2g^2}(C_1^2 + C_1 - 2C_2), \quad (9)$$

where the on-site interaction is parameterized as $U = t/g^2$.

Using the algebraic Bethe ansatz and considering the number of bosons to be M, we obtain the eigenvalues of the transfer matrix $t(u)$ as [49]

$$\Lambda(u) = u^N \prod_{j=1}^{M} \frac{u - \beta_j/U - 1}{u - \beta_j/U} + \epsilon(-t/U)^N \prod_{j=1}^{M} \frac{u - \beta_j/U + 1}{u - \beta_j/U}, \quad (10)$$

where the M Bethe roots $\{\beta_j\}$ should satisfy the Bethe ansatz equations (BAEs)

$$\left(\frac{\beta_j}{-t}\right)^N = \epsilon \prod_{l\neq j}^{M} \frac{\beta_j - \beta_l + U}{\beta_j - \beta_l - U}, \quad j = 1, \ldots, M. \quad (11)$$

Taking the logarithm of BAEs (11), we have

$$N \ln\left(\frac{\beta_j}{-t\sqrt[N]{\epsilon}}\right) = \sum_{l\neq j}^{M} \Theta\left(\frac{U}{\beta_j - \beta_l}\right) + 2i\pi I_j, \quad (12)$$

where $\Theta(z) \equiv 2\mathrm{arctanh}(z)$ and I_j is the quantum number. Each set of integers $\{I_j | j = 1, 2, \ldots, M\}$ characterizes one eigenstate. The eigenvalue of Hamiltonian is

$$E = \sum_{j=1}^{M} \beta_j. \quad (13)$$

The solutions of BAEs (11) or (12) determine the energy spectrum of the Hamiltonian (1) completely.

The superfluid-Mott transition.—First, we consider the case of $\epsilon = 1$. At the limit of $U = 0$, the Bethe roots take $\beta_j = t\exp[i\pi(N + 2l)/N]$ with $l = 1, \ldots, N$. When $U \neq 0$, the Bethe roots can be obtained by solving BAEs (11). To verify the accuracy of our analytical results, we calculate the solutions of BAEs (11) and, thus, obtain all the eigenvalues for a small system with $N = 4$ and $M = 4$.
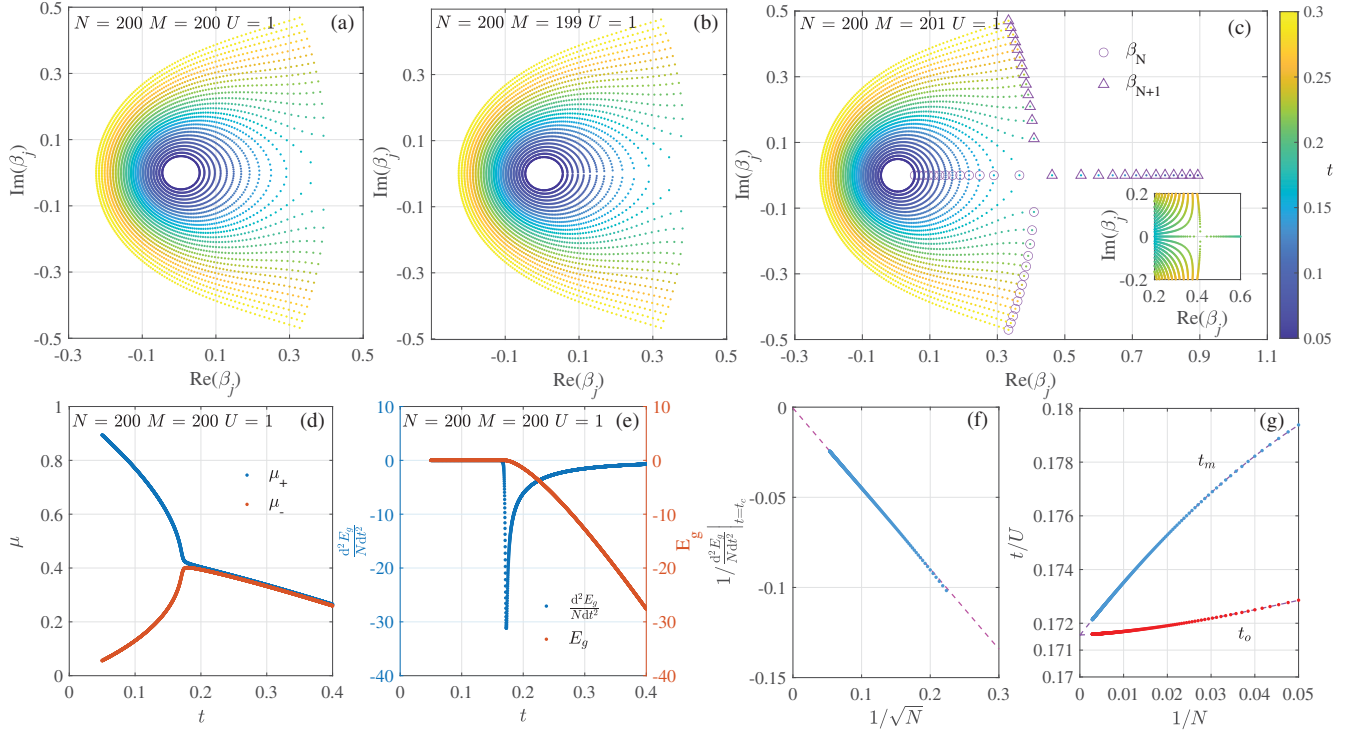
FIG. 1. (a)–(c) Distribution of Bethe roots of the ground state for $U = 1$, $N = 200$, and $M = 200$ (a), 199 (b), and 201 (c) with t varying from 0.3 to 0.05 (the step size is 0.01). The inset in (c) displays a part of the Bethe roots with a finer step size of 0.001. (d) Numerical results of μ_+ and μ_- for the system of $N = M = 200$ and $U = 1$ with t varying from 0.4 to 0.05 (step size 0.0001). (e) The ground state energy E_g (red point) and the second derivative of E_g/N with respect to t/U (blue point) for $N = 200$ and $M = 200$ with t varying from 0.4 to 0.05 (step size 0.0001). (f) The extreme values of (d^2E_g/Ndt^2) plotted against $1/\sqrt{N}$ from $N = 20$ to $N = 350$ ($\rho = 1$). The dashed fitted line is $1/(d^2E_g/Ndt^2) = C_1/\sqrt{N} + C_2$. The fitting parameters are $C_1 = -0.44558$ and $C_2 = -4.9649 \times 10^{-4}$. (g) The value of t_m (blue points) and t_o (red points) versus $1/N$ with $N = 20$–350 ($\rho = 1$). The dashed lines are fitted to determine the values of t_m and t_o as the system size tends to infinity. Fitting results with $N \to \infty$ give $t_m = 0.17155$ and $t_o = 0.17156$.

We compare the results of BAEs with exact diagonalization and confirm that they are consistent (see Supplemental Material [49]).

For the Bose-Hubbard model with integer filling, the system undergoes a superfluid-Mott insulator transition as the ratio of U/t is varied [55]. The critical value of U/t has been determined using various methods such as mean field theory, quantum Monte Carlo simulation [56,57], and density matrix renormalization group method [58].

Now we explore the superfluid-Mott phase transition for the Bose-Hubbard model with unidirectional hopping. We shall focus on the case with unity filling factor $\rho = M/N = 1$ and study its ground state properties. At $U = 0$, the ground state of the system is characterized by N Bethe roots located at $\beta_j = -t$, indicating the condensation of N bosons. As U/t increases from zero, the Bethe roots gradually move away from this point, forming a curve on the complex plane. When U/t exceeds a critical value, the curve closes up and the Bethe roots fill a single ring. To visualize this behavior, we plot the distribution of the Bethe roots of the ground state for various t in Fig. 1(a) while

fixing $U = 1$. It can be seen that, as t decreases, the arc of the curve gradually expands until it closes. When U/t is sufficiently large, the Bethe roots distribute uniformly on a circle with radius t, which is consistent with the hard-core limit of $U/t \to \infty$.

When a boson is removed from the system, we have $M = N - 1$, and the distributions of the Bethe roots are similar to those in the case of $M = N$, as shown in Fig. 1(b). However, adding a boson to the system, i.e., $M = N + 1$, leads to a markedly different behavior in the distribution of Bethe roots when U/t exceeds a critical value. As shown in Fig. 1(c), the two roots with the largest real part, denoted as β_N and β_{N+1}, approach the real axis as t decreases. At $t = t_o$, they coincide. For $t < t_o$, they repel each other and move oppositely along the real axis. If U/t is large enough, we have $\beta_{N+1} \approx \beta_N + U - 2t$, and the other N Bethe roots are distributed on a circle similar to the $M = N$ case.

Next, we reveal that the change in the patterns of Bethe root across t_o is a key indicator of the superfluid-Mott transition. Define $\mu_+ = E_N(\rho N + 1) - E_N(\rho N)$ and $\mu_- = E_N(\rho N) - E_N(\rho N - 1)$, where $E_N(M)$ is the ground
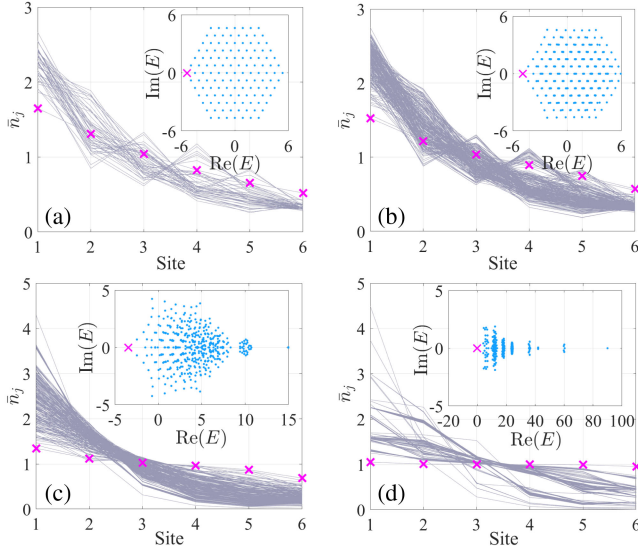
FIG. 2. Exact diagonalization results of the expected values of particle number at each site $\bar{n}_j$ of all eigenstates and the corresponding eigenvalues with $U = 0$ (a), 0.2 (b), 1 (c), and 6 (d), respectively. Each point on the complex plane represents an eigenvalue, while each line corresponds to the particle number distribution of a single state. The ground state particle number distribution and the corresponding energies are marked with crosses. Common parameters: $N = 6, M = 6, t = 1$, and $\epsilon = 0.5$.

state energy for the system with M bosons and N sites. If the system is in the Mott phase, there exists a nonzero gap $\Delta\mu = \mu_+ - \mu_- > 0$, whereas the excitation in the superfluid phase is gapless. As the parameter U/t changes, the position where the energy gap opens or closes marks the superfluid-Mott transition point. In the thermodynamic limit $N\ (M) \to \infty$, the Bethe roots of the ground state distribute continuously. Adding or removing a boson corresponds to adding or removing a Bethe root at the position with the largest real part on the Bethe root distribution curve. Therefore, we have

$$\mu_+ = \text{Re}(\beta_{N+1}), \qquad \mu_- = \text{Re}(\beta_N). \qquad (14)$$

When $t > t_o$, we have $\text{Re}(\beta_{N+1}) = \text{Re}(\beta_N)$ and, thus, $\Delta\mu = 0$. When $t < t_o$, $\Delta\mu = \text{Re}(\beta_{N+1}) - \text{Re}(\beta_N) > 0$. Since $t_o\ (U/t_o)$ defines the position where the gap opens [see Fig. 1(d)], the Mott-superfluid phase transition point can be determined from U/t_o in the thermodynamic limit.

In addition to the Bethe root patterns, the quantum phase transition is also manifested in the ground state energy E_g as a function of U/t (or equally t/U). We demonstrate the change of E_g and the second-order derivative of E_g/N versus the scaled interaction t/U in Fig. 1(e), where E_g shows a steep descent when t exceeds a specific value t_m, accompanied by a peak in $-(d^2 E_g/Ndt^2)$ at t_m. With the finite-size scaling of the maximum of $(d^2 E_g/Ndt^2)$ shown in Fig. 1(f), we get $(d^2 E_g/Ndt^2)|_{t=t_m} \propto \sqrt{N}$, indicating that

the second-order derivative of E_g/N at $t = t_m$ is divergent in the thermodynamic limit.

The finite-size scaling behavior of t_o and t_m is depicted in Fig. 1(g), and it is observed that the critical points determined by the analysis of BAEs and the divergence point of the ground state energy are nearly identical (with $1/N \to 0, |t_m - t_o| < 10^{-5}$). From this, we can extrapolate that the value of the superfluid-Mott phase transition point is $t_c = 0.17155 \pm 10^{-5}$ ($\alpha_c = U/t_c \approx 5.83$). In addition, numerical calculations of the ground state correlation functions provide further support for this result (see Supplemental Material [49]). It is noteworthy that this value is distinct from that in the Bose-Hubbard model with filling $\rho = 1$ where the superfluid-insulator phase transition point is $U_c = 3.28 \pm 0.04$ obtained by the quantum Monte Carlo simulation [59]. For the case with filling $\rho = 2$, similar analysis on the distribution of Bethe roots of the ground state and the ground state energy can be carried out [49]. Our result unveils that the value of superfluid-Mott phase transition point is $t_c = 0.10100 \pm 10^{-5}$.

Non-Hermitian skin effects.—Now, we investigate the effect of boundary parameter ϵ on the eigenstates of the system (1) by considering $\epsilon \neq 1$, which breaks the translation invariance and leads to scale-free NHSE. To comprehend the boundary-induced NHSE in the lattice with unidirectional hopping, it is instructive to see the noninteracting limit of $U = 0$ [60], in which all eigenstates accumulated asymmetrically near the boundaries and exhibit NHSE [see Fig. 2(a)]. From the BAEs (11), for the Bethe roots pattern or the energy spectrum, the parameter value $\{t, \epsilon\}$ is equivalent to $\{t/\sqrt[N]{\epsilon}, 1\}$. For a finite nonzero ϵ, when $N \to \infty$, $\sqrt[N]{\epsilon} \to 1$ and all the eigenvalues are equal to those of the periodic boundary case. It means that ϵ does not change the critical point t_c in the thermodynamic limit.

Next, we demonstrate that the NHSE exists in the interacting system based on the exact solution. Using the coordinate Bethe ansatz method, the eigenstates of the system can be written out explicitly:

$$|\Psi\rangle_m = \sum_{x_1,\dots,x_M=1}^{N} \psi(x_1, \dots, x_M) b_{x_1}^\dagger \dots b_{x_M}^\dagger |0\rangle, \qquad (15)$$

where the subscript m takes the values from 1 to the dimensional of Hilbert space $(N + M - 1)!/[(N - 1)!M!]$, $\psi(x_1, \dots, x_M)$ is the wave function

$$\psi = \sum_{p,q} A_p(q) \prod_{j=1}^{M} \left(\frac{\beta_{p_j}}{-t}\right)^{x_{q_j}} \theta(x_{q_1} \leq \dots \leq x_{q_M}) \qquad (16)$$

with $p = \{p_1, \dots, p_M\}$ and $q = \{q_1, \dots, q_M\}$ being the permutations of $\{1, \dots, M\}$, $\theta(x_{q_1} \leq \dots \leq x_{q_M})$ is the generalized step function, which is one in the noted regime and zero in the others, and $|0\rangle$ is the vacuum state.

The amplitude A_p satisfies

$$\frac{A_{p_1 \dots p_{j+1} p_j \dots p_M}}{A_{p_1 \dots p_j p_{j+1} \dots p_M}} = \frac{\beta_{p_{j+1}} - \beta_{p_j} + U}{\beta_{p_{j+1}} - \beta_{p_j} - U}. \quad (17)$$

Each set of Bethe roots $\{\beta_j\}$ of BAEs (11) completely determines one eigenstate.

The expected values of particle number operator at the jth site $\bar{n}_j = {}_m\langle\Psi|n_j|\Psi\rangle_m$ for all the eigenstates are shown in Figs. 2(b)–2(d), at different values of U while t is fixed to 1. It is shown that the distributions for most eigenstates are localized asymmetrically around the boundary, exhibiting the characters of NHSE. This can be understood directly by analyzing the properties of wave functions. Multiplying the M BAEs (11), we have

$$\prod_{j=1}^{M} \left|\frac{\beta_j}{t}\right| = \epsilon^{M/N}, \quad (18)$$

which gives that

$$|\psi(x_1 + 1, \dots, x_M + 1)| = \epsilon^{M/N}|\psi(x_1, \dots, x_M)|, \quad (19)$$

where $x_j < N$. For the periodic system with $\epsilon = 1$, the wave function has translational symmetry so that the particle number distribution is uniform. With $\epsilon \neq 1$, the translational symmetry is broken. Because of the factor $\epsilon^{M/N}$, the wave function will decay if $\epsilon < 1$ or increase if $\epsilon > 1$ along the sites. Localization lengths of the skin states at $U = 0$ are proportional to the system size and are actually the so-called scale-free localized states [23]. The property (18) is independent on the value of t/U. As shown in Figs. 2(b) and 2(c), the NHSE still survives when interaction is considered. When U is large enough, the Mott phase emerges and the skin effect of the ground state is suppressed as shown in Fig. 2(d). Particularly, the density distribution of a Mott state is uniformly distributed in the thermodynamical limit, and, thus, the NHSE is completely suppressed. This can be manifested from our numerical results (see Supplemental Material [49]) and also the analytical expression of the ground state wave function in the limit of $U \to \infty$ given by $|\Psi\rangle_G = b_1^\dagger b_2^\dagger \dots b_N^\dagger|0\rangle$. In [49], we numerically calculate the average deviation of the uniform distribution defined as $\delta = (1/N)\sum_{j=1}^{N}|\bar{n}_j - \rho|$. Finite-size analysis of our numerical results indicates that δ approaches zero in the limit of $N \to \infty$ for $t/U \leq 0.17$, whereas it approaches a nonzero value for $t/U \geq 0.18$. These numerical results suggest that the skin effect of a Mott state is completely suppressed in the thermodynamical limit.

Summary and outlook.—In the framework of the quantum inverse scattering method, we proved the integrability of the Bose-Hubbard model with unidirectional hopping and derived the Bethe ansatz equations for the system.

Based on the exact solution, we investigated the energy spectrum and distribution of Bethe roots of the ground state, which allows us to identify the existence of a superfluid-Mott insulating transition for integer fillings. Furthermore, we studied the effect of boundary parameter ϵ on the system and demonstrated the presence of NHSE when ϵ departs from 1. We also elucidated the effect of interaction on NHSE and showed that the NHSE is completely suppressed for the Mott insulator state in the thermodynamic limit. Our work introduces a new class of integrable models without Hermitian correspondence and sheds light on the interplay between interaction and NHSE. Additionally, our study provides a benchmark for testing numerical techniques developed for non-Hermitian many-body systems.

Theoretically, it has been unveiled that the combination of loss and multichannel interference with tunable phases can generate nonreciprocal hopping and even unidirectional transmission [61]. Dissipative chain model with nonreciprocal hopping has been implemented in cold atomic optical lattices [62], where nonreciprocal hopping is effectively generated by introducing an auxiliary lattice with on-site loss [61–63]. Therefore, the Bose-Hubbard model with unidirectional hopping is principally realizable in current cold atomic experiments.

*schen@iphy.ac.cn
[1] E. H. Lieb and W. Liniger, Exact analysis of an interacting Bose gas. I. The general solution and the ground state, Phys. Rev. **130**, 1605 (1963).
[2] E. H. Lieb, Exact analysis of an interacting Bose gas. II. The excitation spectrum, Phys. Rev. **130**, 1616 (1963).
[3] C. N. Yang, Some exact results for the many-body problem in one dimension with repulsive delta-function interaction, Phys. Rev. Lett. **19**, 1312 (1967).
[4] M. Gaudin, Un systeme a une dimension de fermions en interaction, Phys. Lett. **24A**, 55 (1967).
[5] E. H. Lieb and F. Y. Wu, Absence of Mott transition in an exact solution of the short-range, one-band model in one dimension, Phys. Rev. Lett. **20**, 1445 (1968).
[6] Xi-Wen Guan, Murray T. Batchelor, and Chaohong Lee, Fermi gases in one dimension: From Bethe ansatz to experiments, Rev. Mod. Phys. **85**, 1633 (2013).

[7] C. M. Bender and S. Boettcher, Real spectra in non-Hermitian Hamiltonians having $\mathcal{PT}$ symmetry, Phys. Rev. Lett. **80**, 5243 (1998).

[8] C. M. Bender, Making sense of non-Hermitian Hamiltonians, Rep. Prog. Phys. **70**, 947 (2007).

[9] E. J. Bergholtz, J. C. Budich, and F. K. Kunst, Exceptional topology of non-Hermitian systems, Rev. Mod. Phys. **93**, 015005 (2021).

[10] Y. Ashida, Z. Gong, and Masahito Ueda, Non-Hermitian physics, Adv. Phys. **69**, 3 (2020).

[11] Z. Gong, Y. Ashida, K. Kawabata, K. Takasan, S. Higashikawa, and M. Ueda, Topological phases of non-Hermitian systems, Phys. Rev. X **8**, 031079 (2018).

[12] C.-H. Liu, H. Jiang, and S. Chen, Topological classification of non-Hermitian systems with reflection symmetry, Phys. Rev. B **99**, 125103 (2019).

[13] K. Kawabata, K. Shiozaki, M. Ueda, and M. Sato, Symmetry and topology in non-Hermitian physics, Phys. Rev. X **9**, 041015 (2019).

[14] H. Zhou and J. Y. Lee, Periodic table for topological bands with non-Hermitian symmetries, Phys. Rev. B **99**, 235112 (2019).

[15] C.-H. Liu and S. Chen, Topological classification of defects in non-Hermitian systems, Phys. Rev. B **100**, 144106 (2019).

[16] C.-H. Liu, H. Hu, and S. Chen, Symmetry and topological classification of Floquet non-Hermitian systems, Phys. Rev. B **105**, 214305 (2022).

[17] S. Yao and Z. Wang, Edge states and topological invariants of non-Hermitian systems, Phys. Rev. Lett. **121**, 086803 (2018).

[18] F. K. Kunst, E. Edvardsson, J. C. Budich, and E. J. Bergholtz, Biorthogonal bulk-boundary correspondence in non-Hermitian systems, Phys. Rev. Lett. **121**, 026808 (2018); Phys. Rev. B **99**, 201103(R) (2019).

[19] C. H. Lee and R. Thomale, Anatomy of skin modes and topology in non-Hermitian systems, Phys. Rev. B **99**, 201103(R) (2019).

[20] K. Yokomizo and S. Murakami, Non-Bloch band theory of non-Hermitian systems, Phys. Rev. Lett. **123**, 066404 (2019).

[21] K. Zhang, Z. Yang, and C. Fang, Correspondence between winding numbers and skin modes in non-Hermitian systems, Phys. Rev. Lett. **125**, 126402 (2020).

[22] N. Okuma, K. Kawabata, K. Shiozaki, and M. Sato, Topological origin of non-Hermitian skin effects, Phys. Rev. Lett. **124**, 086801 (2020).

[23] L. Li, C. H. Lee, and J. Gong, Impurity induced scale-free localization, Commun. Phys. **4**, 42 (2021).

[24] K. Yokomizo and S. Murakami, Scaling rule for the critical non-Hermitian skin effect, Phys. Rev. B **104**, 165117 (2021).

[25] C.-X. Guo, X. Wang, H. Hu, and S. Chen, Accumulation of scale-free localized states induced by local non-Hermiticity, Phys. Rev. B **107**, 134121 (2023).

[26] B. Li, H.-R. Wang, F. Song, and Z. Wang, Scale-free localization and $\mathcal{PT}$ symmetry breaking from local non-Hermiticity, Phys. Rev. B **108**, L161409 (2023).

[27] P. Molignini, O. Arandes, and E. J. Bergholtz, Anomalous skin effects in disordered systems with a single non-Hermitian impurity, Phys. Rev. Res. **5**, 033058 (2023).

[28] D.-W. Zhang, Y.-L. Chen, G.-Q. Zhang, L.-J. Lang, Z. Li, and S.-L. Zhu, Skin superfluid, topological Mott insulators, and asymmetric dynamics in an interacting non-Hermitian Aubry-André-Harper model, Phys. Rev. B **101**, 235150 (2020).

[29] S.-B. Zhang, M. M. Denner, T. Bzdusek, M. A. Sentef, and T. Neupert, Symmetry breaking and spectral structure of the interacting Hatano-Nelson model, Phys. Rev. B **106**, L121102 (2022).

[30] F. Alsallom, L. Herviou, O. V. Yazyev, and M. Brzezińska, Fate of the non-Hermitian skin effect in many-body fermionic systems, Phys. Rev. Res. **4**, 033122 (2022).

[31] Takahiro Fukui and Norio Kawakami, Breakdown of the Mott insulator: Exact solution of an asymmetric Hubbard model, Phys. Rev. B **58**, 16051 (1998).

[32] L. Pan, X. Wang, X. Cui, and S. Chen, Interaction-induced dynamical $\mathcal{PT}$-symmetry breaking in dissipative Fermi-Hubbard models, Phys. Rev. A **102**, 023306 (2020).

[33] T. Liu, J. J. He, T. Yoshida, Z.-L. Xiang, and F. Nori, Non-Hermitian topological Mott insulators in 1D fermionic superlattices, Phys. Rev. B **102**, 235151 (2020).

[34] Zhihao Xu and Shu Chen, Topological Bose-Mott insulators in one-dimensional non-Hermitian superlattices, Phys. Rev. B **102**, 035153 (2020).

[35] Zuo Wang, Li-Jun Lang, and Liang He, Emergent Mott insulators and non-Hermitian conservation laws in an interacting bosonic chain with noninteger filling and non-reciprocal hopping, Phys. Rev. B **105**, 054315 (2022).

[36] T. Yoshida, K. Kudo, H. Katsura, and Y. Hatsugai, Fate of fractional quantum Hall states in open quantum systems: Characterization of correlated topological states for the full Liouvillian, Phys. Rev. Res. **2**, 033428 (2020).

[37] Tsuneya Yoshida and Yasuhiro Hatsugai, Reduction of one-dimensional non-Hermitian point-gap topology by interactions, Phys. Rev. B **106**, 205147 (2022).

[38] Kohei Kawabata, Ken Shiozaki, and Shinsei Ryu, Many-body topology of non-Hermitian systems, Phys. Rev. B **105**, 165137 (2022).

[39] M. J. Colbrook, B. Roman, and A. C. Hansen, How to compute spectra with error control, Phys. Rev. Lett. **122**, 250201 (2019).

[40] C.-X. Guo, C.-H. Liu, X.-M. Zhao, Y. Liu, and S. Chen, Exact solution of non-Hermitian systems with generalized boundary conditions: Size-dependent boundary effect and fragility of the skin effect, Phys. Rev. Lett. **127**, 116801 (2021).

[41] T. C. Choy and F. D. M. Haldane, Failure of Bethe-Ansatz solutions of generalisations of the Hubbard chain to arbitrary permutation symmetry, Phys. Lett. **90A**, 83 (1982).

[42] M. P. A. Fisher, P. B. Weichman, G. Grinstein, and D. S. Fisher, Boson localization and the superfluid-insulator transition, Phys. Rev. B **40**, 546 (1989).

[43] Masaya Nakagawa, Norio Kawakami, and Masahito Ueda, Exact Liouvillian spectrum of a one-dimensional dissipative Hubbard model, Phys. Rev. Lett. **126**, 110404 (2021).

[44] P. Kattel, P. R. Pasnoori, and N. Andrei, Exact solution of a non-Hermitian $\mathcal{PT}$-symmetric Heisenberg spin chain, J. Phys. A **56**, 325001 (2023).

[45] L. Mao, Y. Hao, and L. Pan, Non-Hermitian skin effect in one-dimensional interacting Bose gas, Phys. Rev. A **107,** 043315 (2023).

[46] H.-R. Wang, B. Li, F. Song, and abd Z. Wang, Scale-free non-Hermitian skin effect in a boundary-dissipated spin chain, SciPost Phys. **15,** 191 (2023).

[47] V. E. Korepin, A. G. Izergin, and N. M. Bogoliubov, *Quantum Inverse Scattering Method, Correlation Functions and Algebraic Bethe Ansatz* (Cambridge University Press, Cambridge, England, 1993).

[48] Y. Wang, W.-L. Yang, J. Cao, and K. Shi, *Off-Diagonal Bethe Ansatz for Exactly Solvable Models* (Springer, New York, 2015).

[49] See Supplemental Material at http://link.aps.org/supplemental/10.1103/PhysRevLett.132.086502 for (I) the detailed procedures of deriving the Bethe ansatz equations by the algebraic Bethe ansatz method, (II) the details for the solutions of Bethe roots, (III) more numerical analysis on the superfluid-Mott transition, (IV) discussion on the case of $\rho = 2$, and (V) numerical analysis on the suppression of the skin effect. This includes Refs. [50–54].

[50] V. B. Kuznetsov and A. V. Tsiganov, A special case of Neumann's system and the Kowalewski-Chaplygin-Goryachev top, J. Phys. A **22,** L73 (1989).

[51] F. D. M. Haldane, Effective Harmonic-fluid approach to low-energy properties of one-dimensional quantum fluids, Phys. Rev. Lett. **47,** 1840 (1981).

[52] T. Giamarchi and H. J. Schulz, Correlation functions of one-dimensional quantum systems, Phys. Rev. B **39,** 4620 (1989).

[53] T. D. Kühner, S. R. White, and H. Monien, One-dimensional Bose-Hubbard model with nearest-neighbor interaction, Phys. Rev. B **61,** 12474 (2000).

[54] S. Ejima, H. Fehske, and F. Gebhard, Dynamic properties of the one-dimensional Bose-Hubbard model, Europhys. Lett. **93,** 30002 (2011).

[55] M. Greiner, O. Mandel, T. Esslinger, T. W. HÄansch, and I. Bloch, Quantum phase transition from a superfluid to a Mott insulator in a gas of ultracold atoms, Nature (London) **415,** 39 (2002).

[56] R. T. Scalettar, G. G. Batrouni, and G. T. Zimanyi, Localization in interacting, disordered, Bose systems, Phys. Rev. Lett. **66,** 3144 (1991).

[57] G. G. Batrouni and R. T. Scalettar, World-line quantum Monte Carlo algorithm for a one-dimensional Bose model, Phys. Rev. B **46,** 9051 (1992).

[58] T. D. Kühner and H. Monien, Phases of the one-dimensional Bose-Hubbard model, Phys. Rev. B **58,** R14741 (1998).

[59] L. Pollet, C. Kollath, U. Schollwock, and M. Troyer, Mixture of bosonic and spin-polarized fermionic atoms in an optical lattice, Phys. Rev. A **77,** 023608 (2008).

[60] L. Su, C.-X. Guo, Y. Wang, L. Li, X. Ruan, Y. Du, S. Chen, and D. Zheng, Observation of size-dependent boundary effects in non-Hermitian electric circuits, Chin. Phys. B **32,** 038401 (2023).

[61] X. Huang, C. Lu, C. Liang, H. Tao, and Y.-C. Liu, Loss-induced nonreciprocity, Light. Light. **10,** 30 (2021).

[62] Q. Liang, D. Xie, Z. Dong, H. Li, H. Li, B. Gadway, W. Yi, and B. Yan, Dynamic signatures of non-Hermitian skin effect and topology in ultracold Atoms, Phys. Rev. Lett. **129,** 070401 (2022).

[63] S. Lapp, J. Ang'ong'a, F. A. An, and B. Gadway, Engineering tunable local loss in a synthetic lattice of momentum states, New J. Phys. **21,** 045006 (2019).